Taylor dispersion of gyrotactic swimming micro-organisms in a linear flow

N. A. Hill
Department of Mathematics, University of Glasgow, Glasgow G12 8QW, United Kingdom

M. A. Bees
Department of Mathematics and Statistics, University of Surrey, Guildford, Surrey GU2 7XH, United Kingdom

(Received 26 June 2001; accepted 10 January 2002; published 18 June 2002)

The theory of generalized Taylor dispersion for suspensions of Brownian particles is developed to study the dispersion of gyrotactic swimming micro-organisms in a linear shear flow. Such creatures are bottom-heavy and experience a gravitational torque which acts to right them when they are tipped away from the vertical. They also suffer a net viscous torque in the presence of a local vorticity field. The orientation of the cells is intrinsically random but the balance of the two torques results in a bias toward a preferred swimming direction. The micro-organisms are sufficiently large that Brownian motion is negligible but their random swimming across streamlines results in a mean velocity together with diffusion. As an example, we consider the case of vertical shear flow and calculate the diffusion coefficients for a suspension of the alga *Chlamydomonas nivalis*. This rational derivation is compared with earlier approximations for the diffusivity. © *2002 American Institute of Physics.* [DOI: 10.1063/1.1458003]

I. INTRODUCTION

Many swimming micro-organisms, e.g., single-celled algae and bacteria, swim randomly with a bias toward a preferred direction. The bias may be in response to a chemical gradient (chemotaxis), light (phototaxis), upwards (negative gravitaxis), or a combination of these and other taxes. Suspensions of such creatures often form ordered, large scale ''bioconvection'' patterns, which are manifest as variations in the concentration of the micro-organisms throughout the suspension. The patterns occur because the cells are very active swimmers and are also 5%–10% denser than the suspending fluid (essentially water). Where the cells aggregate, the bulk suspension is more dense than surrounding regions and tends to sink driving bulk circulation which reinforces the aggregation of the cells. For further details, see the review by Pedley and Kessler[1] and Refs. 2–22. Continuum theories of bioconvection require knowledge of the mean swimming velocity $\overline{\mathbf{U}}$ and the diffusion tensor due to swimming $\overline{\mathsf{D}}$, which depend on the local fluid velocity and fluid velocity gradient.

In the absence of light, many cells tend to swim upwards in otherwise still water because they are bottom-heavy or because there is an anterior–posterior asymmetry in their body shape.[23] In either case, local shear flows impose a viscous torque, $\boldsymbol{\tau}_v$, on the cell tipping it away from the vertical, which in turn generates a counterbalancing gravitational torque, $\boldsymbol{\tau}_g$. These two competing torques impose a bias on the cell's random motion that was termed gyrotaxis by Kessler.[8] Hill and Häder[18] showed that individual single-celled algae, e.g., the common algae *Chlamydomonas nivalis* and *Peridinium gatunense*, swim with constant speed and vary their orientation, thus executing a random walk guided by gyrotaxis.

Pedley and Kessler[16] developed a continuum model in which the randomness in the cell swimming direction, $\mathbf{p}$, is accounted for by requiring that the probability density function for $\mathbf{p}$ satisfies a Fokker–Planck equation analagous to that obtained for suspensions of colloidal particles subject to rotational Brownian motion.[24] The coefficients in the Fokker–Planck equation for both the deterministic torques and the rotational diffusivity, d_r, have been calculated by Hill and Häder[18] for *C. nivalis* and *P. gatunense*, and could be measured for other micro-organisms in principle. $\overline{\mathbf{U}}$ and $\overline{\mathsf{D}}$ can be derived from the statistical moments of $\mathbf{p}$. $\overline{\mathbf{U}}$ is straightforward to calculate but $\overline{\mathsf{D}}$ is not. In order to make further analytical progress, Pedley and Kessler[16] used the approximation that

$$\overline{\mathsf{D}} \approx V_s^2 \tau \,\mathrm{var}(\mathbf{p}), \tag{1}$$

where the correlation time τ is a parameter estimated from experimental data. Asymptotic results were obtained for small values of the local rate of strain. Bees *et al.*[19] extended the analysis of this approximation to cover all strain rates. Even so, the approximation is *ad hoc* and in this paper we develop further the theory of generalized Taylor dispersion for orientable Brownian particles due to Frankel and Brenner,[24,25] in order to calculate the dispersal of swimming micro-organisms in such a flow. This gives the asymptotic value of $\overline{\mathsf{D}}$ for times $t \gg d_r^{-1}$. Additionally, we assume that the suspension is sufficiently dilute that cell–cell interactions are rare and unimportant, and that the variations in buoyancy in the suspension that drive bioconvection occur on length scales much greater than those under consideration. The example of a linear vertical-shear flow shows how the *ad hoc* approximation used by Bees *et al.*[19] is not correct in the limit as the vorticity becomes large.

II. FORMULATION OF THE GENERALIZED TAYLOR DISPERSION PROBLEM

A. Governing equations

The swimming cells have a typical diameter of 10–20 μm and are too large for Brownian translational diffusion to be significant compared with their translation due to swimming. Furthermore, the sedimentation speed for such microorganisms is but a few percent of their swimming speed so sedimentation can be neglected too. It follows that in a steady linear shear flow, the probability $P(\mathbf{R},\mathbf{p},t|\mathbf{R}',\mathbf{p}')$ of finding a swimming cell at position $\mathbf{R}\equiv(x,y,z)$ with orientation (i.e., swimming direction) $\mathbf{p}$ at time $t>0$, given that it was at position $\mathbf{R}'$ with orientation $\mathbf{p}'$ at time $t=0$, satisfies the probability-flux conservation equation

$$\frac{\partial P}{\partial t}+\nabla_{\mathrm{R}}.\mathbf{J}+\nabla_{\mathrm{p}}.\mathbf{j}=0, \tag{2}$$

where

$$\mathbf{J}=[\mathbf{V}(\mathbf{R}')+(\mathbf{R}-\mathbf{R}').\mathsf{G}+V_{\mathrm{s}}\mathbf{p}]P \tag{3}$$

is the physical-space flux density and

$$\mathbf{j}=\dot{\mathbf{p}}P-d_{\mathrm{r}}\nabla_{\mathrm{p}}P \tag{4}$$

is the orientational-space flux density. $\nabla_{\mathrm{R}}\equiv(\partial/\partial x,\partial/\partial y,\partial/\partial z)\equiv(\partial/\partial x_1,\partial/\partial x_2,\partial/\partial x_3)$. $\mathbf{p}$ is specified by Euler angles θ and ϕ, θ being the angle that $\mathbf{p}$ makes with the vertical z-axis and ϕ the meridional angle that the projection of $\mathbf{p}$ on to the horizontal xy-plane makes with the x-axis. Thus

$$\nabla_{\mathbf{p}}\equiv\hat{\boldsymbol{\theta}}\,\partial/\partial\theta+\hat{\boldsymbol{\phi}}\ \mathrm{cosec}\,\theta\,\partial/\partial\phi, \tag{5}$$

where $\hat{\boldsymbol{\theta}}$ and $\hat{\boldsymbol{\phi}}$ are unit vectors in the θ and ϕ directions. $\{\mathbf{p},\hat{\boldsymbol{\theta}},\hat{\boldsymbol{\phi}}\}$ form a right-handed spherical polar triad in the body of the swimming cell. $\mathbf{V}$ is the fluid velocity and $\mathsf{G}\equiv(\nabla_{\mathrm{R}}\mathbf{V})^T$, i.e., $\mathsf{G}_{ij}\equiv V_{j,i}$ is the (transpose of the) fluid velocity gradient. The cells swim with constant speed V_{s} in the direction of their orientation vector $\mathbf{p}$. The orientational flux $\mathbf{j}$ in (4) contains two terms which represent its deterministic and random components. The data obtained by Hill and Häder[18] for gyrotactic cells in the absence of flow suggest that the stochastic part of $\mathbf{j}$ is well-modeled by a constant rotational diffusivity d_{r}, which is independent of $\mathbf{p}$. The deterministic part of the cells' rate of change of direction is given by

$$\dot{\mathbf{p}}=\frac{1}{2B}[\boldsymbol{k}-(\boldsymbol{k}.\mathbf{p})\mathbf{p}]+\frac{1}{2}\boldsymbol{\Omega}\wedge\mathbf{p}+\alpha_0\mathbf{p}.\mathsf{E}.(1-\mathbf{pp}) \tag{6}$$

(Ref. 19). The first term on the right-hand side of (6) describes the reorientation due to the cells' being bottom-heavy; $\boldsymbol{k}$ is the unit vector in the z-direction vertically upwards and the biological parameter B is the gyrotactic reorientation time scale. The second term represents reorientation due to the viscous torque on the cell caused by the angular velocity, $\boldsymbol{\Omega}\equiv\nabla_{\mathrm{R}}\wedge\mathbf{V}$, of the fluid, and the third term is reorientation due to the rate of strain, $\mathsf{E}\equiv\frac{1}{2}[\nabla_{\mathrm{R}}\mathbf{V}+(\nabla_{\mathrm{R}}\mathbf{V})^{\mathrm{T}}]$, of the linear shear flow. Here we assume that the cell is a spheroid and $\alpha_0=(a^2-b^2)/(a^2+b^2)$ measures the asymmetry of the cell, a being the length of the semi-major axis and b being the length of the semi-minor axis. For spherical cells, $\alpha_0=0$, and the rate of strain does not affect the orientation. The experimentally determined parameters V_{s}, d_{r}, B, and α_0 are mean values averaged over the whole population. We shall assume that the suspension is monodisperse and neglect any effects due to polydispersivity.

This formulation of the Fokker–Planck equation extends that of Pedley and Kessler[1] and makes clear the separate roles of translation in physical space and rotation in orientational space. Note that unlike the case of Brownian particles considered by Frankel and Brenner,[24,25] there is no translational Brownian diffusion. Instead our particles are active swimmers whose orientation changes stochastically.

B. Boundary conditions

In the far field, P will decay away to zero and to ensure that integrals of the statistical moments of P converge, we impose the condition that

$$(P,\mathbf{J},\mathbf{j})|\mathbf{R}-\mathbf{R}'|^m\rightarrow(0,\mathbf{0},\mathbf{0})\ \text{ as }\ |\mathbf{R}-\mathbf{R}'|\rightarrow\infty \quad \text{for } m=0,1,2,... \tag{7}$$

and that P be continuous and single-valued in $\mathbf{p}$ on the unit sphere, S_2. Because P is a probability density function,

$$\int_{R_\infty}\int_{S_2}P\,d^2\mathbf{p}\,d^3\mathbf{R}=1 \quad \text{for all times } t>0, \tag{8}$$

R_∞ being the whole Euclidean space, and we impose the initial condition

$$P=\delta(\mathbf{R}-\mathbf{R}')\,\delta(\mathbf{p}-\mathbf{p}') \quad \text{at} \quad t=0. \tag{9}$$

Thus the initial position and orientation of the cells are specified. This is not restrictive because we shall show that the long-time statistics are independent of the initial conditions.

C. Spatial dispersion

On the bulk or continuum scale, we seek to describe the dispersion of the swimming cells and are interested in only their spatial distribution not their orientation, i.e., we wish to calculate the orientational average probability density function (p.d.f.)

$$\overline{P}(\mathbf{R},t|\mathbf{R}',\mathbf{p}')\equiv\int_{S_2}P(\mathbf{R},\mathbf{p},t|\mathbf{R}',\mathbf{p}')d^2\mathbf{p}. \tag{10}$$

$\overline{P}(\mathbf{R},t|\mathbf{R}',\mathbf{p}')$ satisfies a Fokker–Planck equation of the form

$$\frac{\partial\overline{P}}{\partial t}+\nabla_{\mathrm{R}}.\overline{\mathbf{J}}=0. \tag{11}$$

The asymptotic long-time leading order form of the flux of $\overline{P}$ is

$$\overline{\mathbf{J}}=[\mathbf{V}(\mathbf{R}')+(\mathbf{R}-\mathbf{R}').\mathsf{G}+\overline{\mathbf{U}}]\overline{P}-\overline{\mathsf{D}}.\nabla_{\mathrm{R}}\overline{P}, \tag{12}$$

subject to far-field conditions

$$(\overline{P},\overline{\mathbf{J}})|\mathbf{R}-\mathbf{R}'|^m\rightarrow(0,\mathbf{0})\ \text{ as }\ |\mathbf{R}-\mathbf{R}'|\rightarrow\infty \quad \text{for } m=0,1,2,..., \tag{13}$$

and the initial condition

$$\overline{P} = \delta(\mathbf{R}-\mathbf{R}') \quad \text{at} \quad t=0. \tag{14}$$

The flux is given by (12) provided that the real parts of the eigenvalues of G are zero. This condition is needed so that advection by the fluid motion alone does not lead to exponentially rapid divergence of the position vector of adjacent material points. Thus, for example, straining flows such as $\mathbf{V}=(x,0,-z)^T$ are excluded.[24] The phenomenological constants $\overline{\mathbf{U}}$ and $\overline{\mathsf{D}}$ appearing in (12) can be calculated using generalized Taylor dispersion theory for an unbounded flow.[24,25] They represent a drift velocity and effective diffusivity for the swimming cells. They are defined in terms of the statistical moments

$$\mathsf{M}_m \equiv \int_{R_\infty}\int_{S_2} (\mathbf{R}-\mathbf{R}')^m P\, d^2\mathbf{p}\, d^3\mathbf{R} \quad (m=0,1,2,\ldots) \tag{15}$$

of P, the existence of which is guaranteed by the boundary conditions (13). $\overline{\mathbf{U}}$ is defined by

$$\overline{\mathbf{U}} + \mathbf{V}(\mathbf{R}') = \lim_{t\to\infty}\frac{\delta \mathsf{M}_1}{\delta t} \equiv \lim_{t\to\infty}\left(\frac{d\mathsf{M}_1}{dt} - \mathsf{M}_1\cdot\mathsf{G}\right), \tag{16}$$

where $\delta(.)/\delta t$ is the codeformational (''Oldroyd'') rate of change.[26] Thus $\overline{\mathbf{U}}$ is a drift velocity *relative* to the moving fluid. Similarly, $\overline{\mathsf{D}}$ is given by

$$\begin{aligned}\overline{\mathsf{D}} &= \lim_{t\to\infty}\frac{1}{2}\frac{\delta}{\delta t}(\mathsf{M}_2 - \mathsf{M}_1\mathsf{M}_1) \\ &\equiv \lim_{t\to\infty}\frac{1}{2}\left[\frac{d}{dt}(\mathsf{M}_2-\mathsf{M}_1\mathsf{M}_1) - (\mathsf{M}_2-\mathsf{M}_1\mathsf{M}_1)\cdot\mathsf{G}\right. \\ &\quad \left. - \mathsf{G}^T\cdot(\mathsf{M}_2-\mathsf{M}_1\mathsf{M}_1)\right],\end{aligned} \tag{17}$$

and represents diffusion *relative* to the moving fluid.

An application of generalized Taylor dispersion theory (see the Appendix) shows that $\overline{\mathbf{U}}$ and $\overline{\mathsf{D}}$ can be evaluated from the integrals

$$\overline{\mathbf{U}} = \int_{S_2} P_0^\infty(\mathbf{p}) V_s \mathbf{p}\, d^2\mathbf{p} \tag{18}$$

and

$$\overline{\mathsf{D}} = V_s \int_{S_2} P_0^\infty(\mathbf{p})[\mathbf{B}\mathbf{p}]^{\mathrm{sym}}\, d^2\mathbf{p}. \tag{19}$$

Here $[\ ]^{\mathrm{sym}}$ denotes the symmetric part of the tensor argument and

$$P_0^\infty(\mathbf{p}) = \lim_{t\to\infty} P_0(\mathbf{p},t|\mathbf{R}',\mathbf{p}'), \tag{20}$$

where

$$P_0(\mathbf{p},t|\mathbf{R}',\mathbf{p}') \equiv \int_{R_\infty} P(\mathbf{R},\mathbf{p},t|\mathbf{R}',\mathbf{p}')\, d^3\mathbf{R}. \tag{21}$$

Thus $P_0^\infty(\mathbf{p})$ is the steady long-time p.d.f. for the orientation of the cells. It is continuous and single-valued on S_2, and satisfies

$$\nabla_{\mathrm{p}}\cdot(\dot{\mathbf{p}}P_0^\infty - d_{\mathrm{r}}\nabla_{\mathrm{p}}P_0^\infty) = 0, \tag{22}$$

subject to the normalization condition

$$\int_{S_2} P_0^\infty d^2\mathbf{p} = 1. \tag{23}$$

The definition of $\overline{\mathbf{U}}$ (18) is entirely intuitive, and we see immediately that

$$\overline{\mathbf{U}} \equiv V_s\overline{\mathbf{p}}, \tag{24}$$

i.e., the mean swimming velocity. The definition of $\overline{\mathsf{D}}$ is not so obvious and was first derived for Brownian particles in an unbounded shear flow by Frankel and Brenner.[24] The vector field $\mathbf{B}(\mathbf{p})$ in (19) is defined as

$$\mathbf{B}(\mathbf{p}) = \lim_{t\to\infty}\left(\frac{\overline{\mathbf{P}}_1}{P_0} - \mathsf{M}_1\right), \tag{25}$$

where

$$\overline{\mathbf{P}}_1(\mathbf{p},t|\mathbf{R}',\mathbf{p}') = \int_{R_\infty}(\mathbf{R}-\mathbf{R}')P(\mathbf{R},\mathbf{p},t|\mathbf{R}',\mathbf{p}')d^3\mathbf{R}. \tag{26}$$

Thus $\mathbf{B}(\mathbf{p})$ is the long-time limit of the difference between the average position of the particle, *given that its instantaneous orientation is* $\mathbf{p}$, and its average position *averaged over all values of* $\mathbf{p}$ [see Eq. (15)]. $\mathbf{B}(\mathbf{p})$ satisfies

$$\nabla_{\mathrm{p}}\cdot[\dot{\mathbf{p}}P_0^\infty\mathbf{B} - d_{\mathrm{r}}\nabla_{\mathrm{p}}(P_0^\infty\mathbf{B})] - P_0^\infty\mathbf{B}\cdot\mathsf{G} = P_0^\infty(V_s\mathbf{p}-\overline{\mathbf{U}}) \tag{27}$$

(see the Appendix), subject to the obvious condition

$$\int_{S_2} P_0^\infty\mathbf{B}\, d^2\mathbf{p} = 0. \tag{28}$$

On defining a Péclet number

$$\mathrm{Pe} = G/d_{\mathrm{r}}, \quad \text{where} \quad G = \|\mathsf{G}\|, \tag{29}$$

Eq. (27) becomes

$$\nabla_{\mathrm{p}}\cdot[\mathrm{Pe}\,\hat{\mathbf{p}}\mathbf{b} - \nabla_{\mathrm{p}}\mathbf{b}] - \mathrm{Pe}\,\mathbf{b}.\hat{\mathsf{G}} = P_0^\infty(\mathbf{p}-\overline{\mathbf{p}}), \tag{30}$$

where $\mathbf{b} = P_0^\infty\mathbf{B}d_{\mathrm{r}}/V_s$, $\hat{\mathsf{G}} = \mathsf{G}/G$, and $\hat{\mathbf{p}} = \dot{\mathbf{p}}/G$. Thus to determine $\overline{\mathbf{U}}$ and $\overline{\mathsf{D}}$, we solve Eq. (22) for P_0^∞ and evaluate $\overline{\mathbf{U}} = V_s\overline{\mathbf{p}}$ from the integral (18). After substituting for P_0^∞ and $\overline{\mathbf{p}}$, Eq. (30) is solved for $\mathbf{b}$, subject to the condition

$$\int_{S_2}\mathbf{b}\, d^2\mathbf{p} = 0, \tag{31}$$

and finally $\overline{\mathsf{D}}$ is found from the integral

$$\overline{\mathsf{D}} = \frac{V_s^2}{d_{\mathrm{r}}}\int_{S_2}[\mathbf{b}\mathbf{p}]^{\mathrm{sym}}\, d^2\mathbf{p}, \tag{32}$$

which is derived from (19). Using $\mathbf{b}$ instead of $\mathbf{B}$ simplifies the evaluation of $\overline{\mathsf{D}}$ in the following analysis. Note that $\mathbf{b}$ is dimensionless so that $\overline{\mathsf{D}}$ scales like V_s^2/d_{r}.

III. DISPERSION IN VERTICAL SHEAR FLOW

As an example of the dispersion of gyrotactic micro-organisms and to illustrate the method of solution, we consider the vertical shear flow given by

$$\mathbf{V}=Gz\boldsymbol{i} \tag{33}$$

and suppose that the cells are spherical so that $\alpha_0=0$ and the last term in (6) vanishes. The horizontal unit vectors $\boldsymbol{i}$ and $\boldsymbol{j}$ together with $\boldsymbol{k}$ form a right-handed, mutually orthogonal Cartesian triad. Writing

$$\hat{\mathbf{p}}=\dot{\theta}\hat{\boldsymbol{\theta}}+\dot{\phi}\sin\theta\hat{\boldsymbol{\phi}}, \tag{34}$$

in (6) yields

$$\dot{\theta}=\frac{1}{2}\cos\phi-\frac{\gamma}{2}\sin\theta, \quad \dot{\phi}=-\frac{1}{2}\cot\theta\sin\phi, \tag{35}$$

where $\gamma=1/BG$. Equation (22) for P_0^∞ and (30) for $\mathbf{b}$ then become

$$\mathcal{L}P_0^\infty=0 \tag{36}$$

and

$$\mathcal{L}b_j-\mathrm{Pe}\,b_3\delta_{1j}=P_0^\infty(p_j-\overline{p_j}) \quad (j=1,2,3), \tag{37}$$

where the subscript j denotes the Cartesian components of the vectors. The linear differential operator $\mathcal{L}$ is defined as

$$\mathcal{L}(.)=\frac{\mathrm{Pe}}{2}\Bigg[(\cos\phi-\gamma\sin\theta)\frac{\partial}{\partial\theta}(.)-\cot\theta\sin\phi\frac{\partial}{\partial\phi}(.)-2\gamma\cos\theta(.)\Bigg]-\frac{1}{\sin\theta}\frac{\partial}{\partial\theta}\left(\sin\theta\frac{\partial}{\partial\theta}(.)\right)-\frac{1}{\sin^2\theta}\frac{\partial^2}{\partial\phi^2}(.) \tag{38}$$

and δ_{ij} is the Kronecker delta function.

Equations (36) and (37) are solved by expanding P_0^∞ and $\mathbf{b}$ in spherical harmonics viz.

$$P_0^\infty(\theta,\phi)=\sum_{n=0}^{\infty}\sum_{m=0}^{n}A_n^m\cos m\phi\,P_n^m(\cos\theta) \tag{39}$$

and

$$b_j(\theta,\phi)=\sum_{n=0}^{\infty}\sum_{m=0}^{n}(\beta_{nj}^m\cos m\phi+\gamma_{nj}^m\sin m\phi)P_n^m(\cos\theta) \quad (j=1,2,3), \tag{40}$$

where P_n^m are associated Legendre polynomials[27] and the coefficients β_{nj}^m, γ_{nj}^m and A_n^m depend on the flow field. The symmetry of the flow in this example implies that the expansion of P_0^∞ in (39) requires only even harmonics in ϕ. We further define

$$F_n^m(\theta,\phi)\equiv A_n^m\cos m\phi\,P_n^m(x)\equiv R_n^m(\phi)P_n^m(\cos\theta)\equiv A_n^mQ_n^m(\theta,\phi)$$

and

$$B_{nj}^m(\theta,\phi)\equiv R_{nj}^m(\phi)P_n^m(\cos\theta) \tag{41}$$

$$\equiv[\beta_{nj}^m\cos m\phi+\gamma_{nj}^m\sin m\phi]P_n^m(x) \tag{42}$$

$$\equiv\beta_{nj}^mQ_n^m(\theta,\phi)+\gamma_{nj}^mS_n^m(\theta,\phi), \tag{43}$$

where $x\equiv\cos\theta\Leftrightarrow\partial/\partial\theta=-\sin\theta\,\partial/\partial x$, cf. Eq. (12) in Bees *et al.*[19]

The solution for P_0^∞ now follows exactly that in Ref. 19 (on identifying P_0^∞ with f). Substituting the series (39) into (36) gives

$$\sum_{n=0}^{\infty}\sum_{m=0}^{n}\left\{n(n+1)F_n^m+\frac{1}{2}\mathrm{Pe}\,[(\gamma\sin\theta-\cos\phi)\sin\theta\,R_n^mP_n^{m\prime}-\cot\theta\sin\phi\;R_n^{m\prime}P_n^m-2\gamma\cos\theta F_n^m]\right\}=0, \tag{44}$$

where a prime denotes differentiation with respect to the dependent variable. The normalization condition (23) requires that $A_0^0=1/4\pi$.

The solution for $\mathbf{b}$ proceeds in a similar vein. The series (40) is substituted into (37), which gives

$$\sum_{n=0}^{\infty}\sum_{m=0}^{n}\left(n(n+1)B_{n1}^m+\frac{1}{2}\mathrm{Pe}\,[(\gamma\sin\theta-\cos\phi)\sin\theta\,R_{n1}^mP_n^{m\prime}-\cot\theta\sin\phi\;R_{n1}^{m\prime}P_n^m-2\gamma\cos\theta\;B_{n1}^m]\right)=\sum_{n=0}^{\infty}\sum_{m=0}^{n}\left(\mathrm{Pe}\beta_{n3}^mQ_n^m+\mathrm{Pe}\gamma_{n3}^mS_n^m+\left[\sin\theta\cos\phi-\frac{4\pi}{3}A_1^1\right]A_n^mQ_n^m\right), \tag{45}$$

$$\sum_{n=0}^{\infty}\sum_{m=0}^{n}\left(n(n+1)B_{n2}^m+\frac{1}{2}\mathrm{Pe}\,[(\gamma\sin\theta-\cos\phi)\sin\theta\,R_{n2}^mP_n^{m\prime}-\cot\theta\sin\phi\,R_{n2}^{m\prime}P_n^m-2\gamma\cos\theta\,B_{n2}^m]\right)=\sum_{n=0}^{\infty}\sum_{m=0}^{n}A_n^mQ_n^m\sin\theta\sin\phi, \tag{46}$$

$$\sum_{n=0}^{\infty}\sum_{m=0}^{n}\left(n(n+1)B_{n3}^{m}+\frac{1}{2}\mathrm{Pe}[(\gamma\sin\theta-\cos\phi)\sin\theta R_{n3}^{m}P_{n}^{m\prime}-\cot\theta\sin\phi\,R_{n3}^{m\prime}P_{n}^{m}-2\gamma\cos\theta\,B_{n3}^{m}]\right)=\sum_{n=0}^{\infty}\sum_{m=0}^{n}A_{n}^{m}Q_{n}^{m}\left(\cos\theta-\frac{4\pi}{3}A_{1}^{0}\right). \tag{47}$$

The normalization condition (31) gives

$$\beta_{0j}^{0}=0 \quad (j=1,2,3). \tag{48}$$

The following identities are useful in simplifying (45)–(47):

$$\sin^{2}\theta P_{n}^{m\prime}=[(n+m)P_{n-1}^{m}-n(n-m+1)P_{n+1}^{m}]/(2n+1) \tag{49}$$

and

$$\cos\phi\sin\theta R_{nj}^{m}P_{n}^{m\prime}+\cot\theta\sin\phi R_{nj}^{m\prime}P_{n}^{m}=-\frac{\beta_{nj}^{m}}{2}[Q_{nj}^{m+1}-(n-m+1)(n+m)Q_{nj}^{m-1}]-\frac{\gamma_{nj}^{m}}{2}[S_{nj}^{m+1}-(n-m+1)(n+m)S_{nj}^{m-1}] \tag{50}$$

(see Ref. 19). Equations (44)–(47) were simplified using identities for spherical harmonic functions as in Ref. 19 so that the inner products could be calculated easily. The resulting equations were then truncated to give a set of simultaneous equations for the coefficients A_n^m, β_{nj}^m, and γ_{nj}^m. Using spherical harmonic identities, it can be shown that

$$\overline{\mathbf{p}}=(4\pi/3)(A_{1}^{1},0,A_{1}^{0})^{T} \tag{51}$$

as in Ref. 19 [their Eq. (39)] so that $\overline{\mathbf{U}}=V_s\overline{\mathbf{p}}$ [see (18)] is readily calculated. Similarly,

$$\overline{\mathsf{D}}=\frac{2\pi}{3}\frac{V_s^2}{d_r}\begin{pmatrix}2\beta_{11}^{1} & \beta_{12}^{1}+\gamma_{11}^{1} & \beta_{11}^{0}+\beta_{13}^{1}\\ \beta_{12}^{1}+\gamma_{11}^{1} & 2\gamma_{12}^{1} & \beta_{12}^{0}+\gamma_{13}^{1}\\ \beta_{11}^{0}+\beta_{13}^{1} & \beta_{12}^{0}+\gamma_{13}^{1} & 2\beta_{13}^{0}\end{pmatrix}. \tag{52}$$

These expressions for $\overline{\mathbf{p}}$ and $\overline{\mathsf{D}}$ are important because $\overline{\mathbf{p}}$ and $\overline{\mathsf{D}}$ depend on just a small number of the coefficients, A_n^m, β_{nj}^m and γ_{nj}^m, of P_0^∞ and **b**. The truncated system of equations for the coefficients was constructed and solved analytically using a computer program written in MAPLE using exact arithmetic. (A copy of the code is available from the authors on request.) The coefficients converge rapidly as the order of truncation is increased, as we shall demonstrate. Consequently, in practice, we need only to include terms of fourth order ($n=4$) in the calculation.

It is convenient to rescale the problem to reduce the number of parameters. We define

$$\lambda=1/(2Bd_r), \tag{53}$$

which is fixed and plot $\overline{\mathsf{D}}$ as a function of the "effective vorticity"

$$\zeta=BG \tag{54}$$

instead of Pe and G, as in Ref. 19. In terms of λ and ζ, the equations for P_0^∞ and **b**, (36) and (37), become

$$\mathcal{L}^{*}P_{0}^{\infty}=0 \tag{55}$$

and

$$\mathcal{L}^{*}b_{j}-2\zeta b_{3}\delta_{1j}=P_{0}^{\infty}(p_{j}-\overline{p_{j}})/\lambda \quad (j=1,2,3), \tag{56}$$

and the linear differential operator $\mathcal{L}^*$ is

$$\mathcal{L}^{*}(.)=(\zeta\cos\phi-\sin\theta)\frac{\partial}{\partial\theta}(.)-\zeta\cot\theta\sin\phi\frac{\partial}{\partial\phi}(.)-2\cos\theta(.)-\frac{1}{\lambda\sin\theta}\frac{\partial}{\partial\theta}\left(\sin\theta\frac{\partial}{\partial\theta}(.)\right)-\frac{1}{\lambda\sin^{2}\theta}\frac{\partial^{2}}{\partial\phi^{2}}(.). \tag{57}$$

In order to make comparisons with Ref. 19, we take $\lambda=2.2$, which is typical for a suspension of *C. nivalis*.

IV. RESULTS

In Figs. 1 and 2, we show the behavior of $\overline{\mathbf{p}}$, which gives the direction of the mean swimming velocity (24), as ζ varies. It was shown in Ref. 19 that the approximations for $\overline{\mathbf{p}}$ converge rapidly as n increases from 2 to 4, with orders 3 and 4 being almost indistinguishable. We see that $\overline{\mathbf{p}}$ is vertical when $\zeta=0$ and rotates toward the x axis as ζ increases from 0. $|\overline{\mathbf{p}}|$ and thus $|\overline{\mathbf{U}}|$ decrease monotonically as $|\zeta|$ increases, because P_0^∞ (the steady long-time p.d.f. for the orientation of the cells) becomes more uniform as $|\zeta|$ increases.

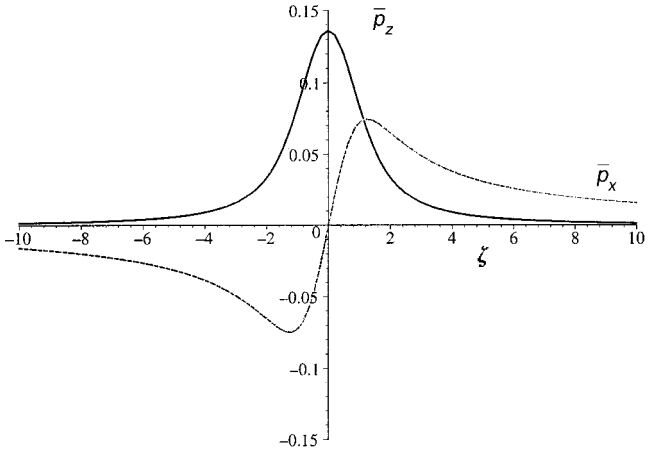

FIG. 1. The variation of the nonzero components of the mean swimming direction $\overline{\mathbf{p}}$ with effective vorticity ζ.

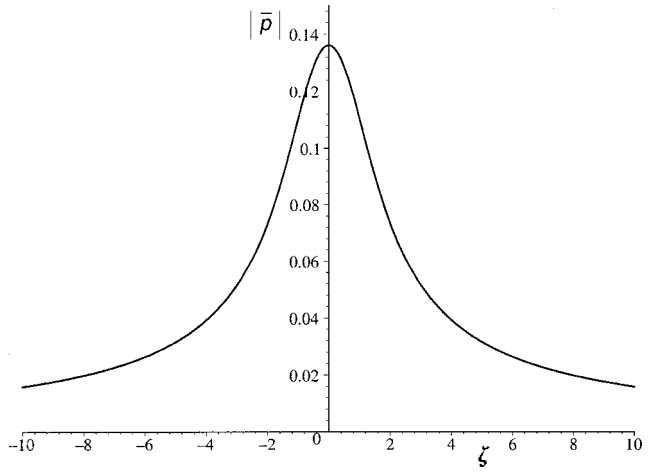

FIG. 2. The variation of the magnitude of the mean swimming direction, $\overline{\mathbf{p}}$, with effective vorticity ζ.

Figure 1 also shows that the combination of the rotation of $\overline{\mathbf{p}}$ and its decrease in magnitude cause $\overline{p_x}$ to increase initially and then decrease as $|\zeta|$ increases.

The nonzero coefficients of the dimensionless effective diffusivity, $\hat{\mathsf{D}}=d_r\overline{\mathsf{D}}/V_s^2$, are plotted as functions of ζ in Figs. 3–6. They show successive approximations as m is increased from 2 to 4. The graphs show that we obtain good convergence across the whole range of values of ζ by including the fourth-order terms. To understand the behavior of $\hat{\mathsf{D}}$, its eigenvalues $\hat{\mathsf{D}}_i$ $(i=1,2,3)$ are plotted as functions of ζ in Fig. 7. They are labeled such that the eigenvectors corresponding to $\hat{\mathsf{D}}_1$, $\hat{\mathsf{D}}_2$, and $\hat{\mathsf{D}}_3$ are parallel to $\boldsymbol{i}$, $\boldsymbol{j}$, and $\boldsymbol{k}$, respectively, when $\zeta=0$.

First note that $\hat{\mathsf{D}}$ is anisotropic. In the absence of flow, $\hat{\mathsf{D}}_1=\hat{\mathsf{D}}_2$ and they are about four times greater than $\hat{\mathsf{D}}_3$. Next consider what happens as ζ increases from 0. (The case when $\zeta<0$ is explained by the obvious symmetries.) There are two main competing effects. As ζ increases from 0 to 1, $P_0^{\infty}(\mathbf{p})$

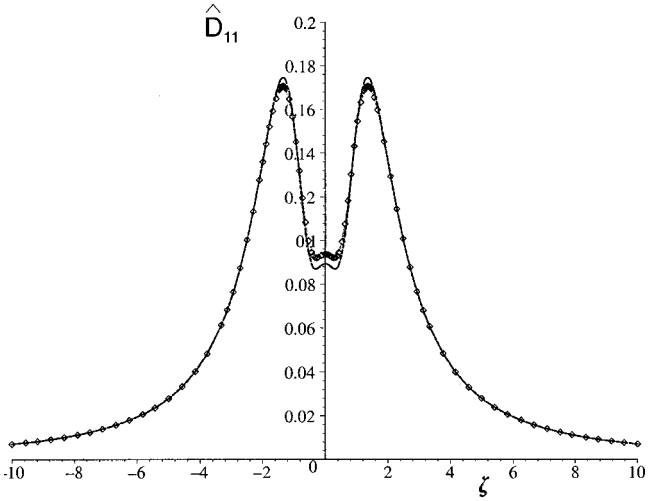

FIG. 3. Graph of $\hat{\mathsf{D}}_{11}$ as a function of the effective vorticity ζ for approximations of order 2, 3, and 4. Dashed line=order 2, solid line=order 3, and diamonds=order 4 solution.

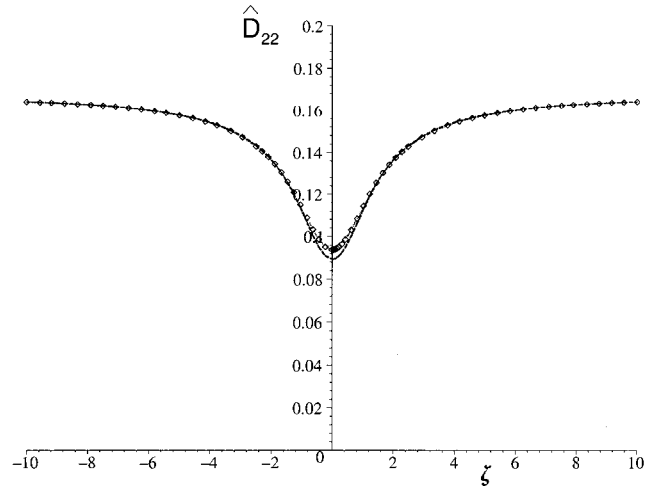

FIG. 4. Graph of $\hat{\mathsf{D}}_{22}$ as a function of the effective vorticity ζ for approximations of order 2, 3, and 4. Dashed line=order 2, solid line=order 3, and diamonds=order 4 solution.

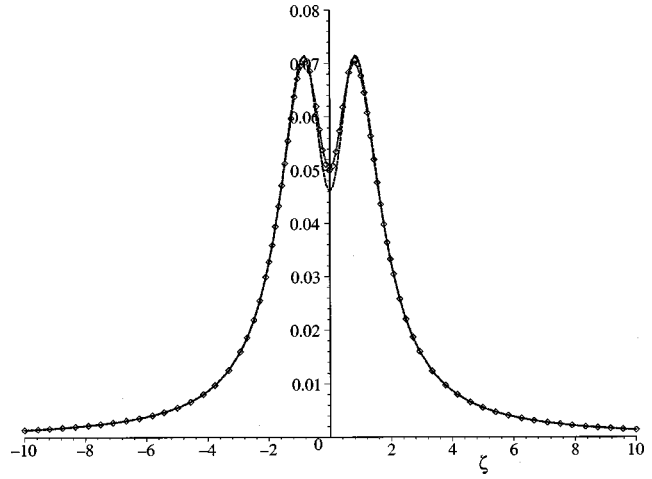

FIG. 5. Graph of $\hat{\mathsf{D}}_{33}$ as a function of the effective vorticity ζ for approximations of order 2, 3, and 4. Dashed line=order 2, solid line=order 3, and diamonds=order 4 solution.

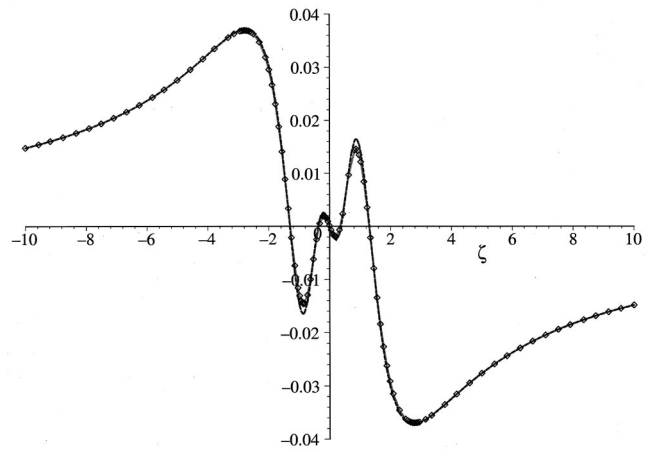

FIG. 6. Graph of $\hat{\mathsf{D}}_{13}=\hat{\mathsf{D}}_{31}$ as a function of the effective vorticity ζ for approximations of order 2, 3, and 4. Dashed line=order 2, solid line=order 3, and diamonds=order 4 solution.

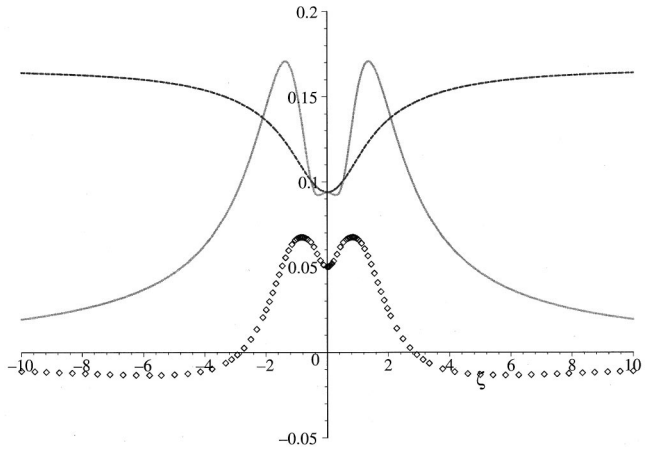

FIG. 7. Plot of the eigenvalues of $\hat{\mathsf{D}}$ as functions of the effective vorticity ζ.

becomes less peaked and dispersion increases, resulting in an increase in all three eigenvalues, except for a small initial decrease in $\hat{\mathsf{D}}_1$. For values of $\zeta>1$, cells ''tumble'' about the *y*-axis in the sense that the deterministic torque balance (6) has no steady solution. As ζ increases beyond 1, the tumbling of the cells becomes faster, they tend to swim in tighter and tighter loops, and the autocorrelation times for the *x* and *z* components of the velocity fluctuations about the mean shorten. As a result, $\hat{\mathsf{D}}_1$ and $\hat{\mathsf{D}}_3\to 0$ as $\zeta\to\infty$. Since the cells tumble only about the *y*-axis, tumbling does not affect the autocorrelation times for the *y*-component of the velocity fluctuations so that $\hat{\mathsf{D}}_2$ increases monotonically and tends to a finite limit as $\zeta\to\infty$. We also note that $\hat{\mathsf{D}}_3$ is negative for values of $\zeta>2.8$. The possibility of negative eigenvalues was recognized by Frankel and Brenner[24,25] and arises because the Taylor dispersion mechanism is coupled to the distortion due to the flow. An alternative definition for the diffusivity is

$$\bar{\mathsf{D}}=\frac{V_s^2}{d_r}\int_{S_2}[\mathbf{bp}+\mathrm{Pe}\,\mathbf{b}\hat{\mathbf{B}}\cdot\hat{\mathsf{G}}]^{\mathrm{sym}}d^2\mathbf{p}\quad\text{where}\quad\hat{\mathbf{B}}\equiv d_r\mathbf{B}/V_s,$$

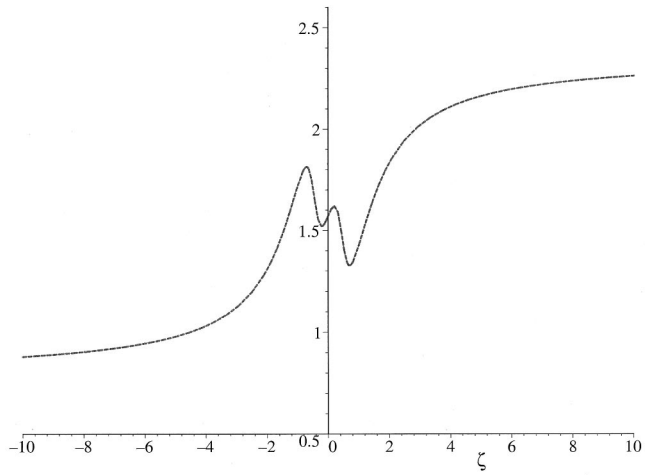

FIG. 8. Graph of change in the orientation of the principal eigenvector, $\mathbf{e}_1$, of $\hat{\mathsf{D}}$ as ζ varies. Θ is the angle that $\mathbf{e}_1$ makes with the vertical *z* axis.

cf. Eq. (32). This is positive definite and still gives the long-time matching of the moments of P in the co-deformational reference frame. When the behavior of $\hat{\mathsf{D}}_1$ and $\hat{\mathsf{D}}_3$ as $\zeta\to\infty$ is compared with the results from Refs. 16 and 19, the limitations of their approximation (1) are exposed. For this example, they erroneously predict that $\bar{\mathsf{D}}=O(V_s^2\tau)$ in the same limit. This is because their approximation is proportional to var($\mathbf{p}$), which tends to I, the identity matrix, instead of vanishing.

Figure 8 shows the orientation of the principal eigenvector, $\mathbf{e}_1$ corresponding to $\hat{\mathsf{D}}_1$, as ζ varies. It lies in the *xz*-plane, and lies along the horizontal *x* axis in the absence of flow. As ζ increases from 0, $\mathbf{e}_1$ first dips a little below the *x*-axis then reverses its sense of rotation until it is again horizontal at $\zeta\approx 0.4$. This initial behavior appears to be associated with the slight decrease in $\hat{\mathsf{D}}_1$ for the same values of ζ. As ζ increases further from 0.4 to about 1.0, $\mathbf{e}_1$ continues to rotate upwards in the opposite sense to the rotation of $\overline{\mathbf{p}}$. Once tumbling occurs at values of $\zeta>1$, $\mathbf{e}_1$ rotates downwards as ζ increases, eventually pointing below the *x* axis for values of $\zeta>2$.

V. CONCLUSIONS

We have extended generalized Taylor dispersion theory to gyrotactic swimming microorganisms and derived the first rational expressions for the diffusion coefficients of suspensions of such creatures in a flow. The results are valid in the long time limit $t\gg d_r^{-1}$. This work and its extensions to other types of micro-organism swimming behavior can be applied to calculations of pattern formation by bioconvection in bulk suspensions. Of particular interest is the fact that dispersion occurs even when Brownian translational motion is negligible because of the size of the cells. It is the stochastic reorientation of the swimming cells that leads to dispersion.

ACKNOWLEDGMENT

N.A.H. gratefully acknowledges the support of the U.K. EPSRC (Grant Reference No. GR/J75470) for part of this work.

APPENDIX: GENERALIZED TAYLOR DISPERSION THEORY

The results of generalized Taylor dispersion theory can be derived for gyrotactic swimming micro-organisms by establishing a direct correspondence with the form of the flux terms in the Fokker–Planck equation (2) for $P(\mathbf{R},\mathbf{p},t|\mathbf{R}',\mathbf{p}')$ used by Frankel and Brenner[25] for spheroidal Brownian particles subject to external forces in an unbounded homogeneous linear shear flow. The flux terms used by these authors are (in our notation)

$$\mathbf{J}=[\mathbf{V}(\mathbf{R}')+(\mathbf{R}-\mathbf{R}').\mathsf{G}+\mathsf{M}(\mathbf{p}).\mathbf{F}]P-\mathsf{D}_T(\mathbf{p}).\boldsymbol{\nabla}_R P \tag{A1}$$

and

$$\mathbf{j}=\dot{\mathbf{p}}P-d_r\boldsymbol{\nabla}_p P, \tag{A2}$$

where

$$\dot{\mathbf{p}} = \tfrac{1}{2}\boldsymbol{\Omega}\wedge\mathbf{p} + \alpha_0 \mathbf{p}.\mathsf{E}.(\mathsf{I}-\mathbf{pp}). \tag{A3}$$

[$\mathbf{p} \mapsto \mathbf{e}$ in Frankel and Brenner's[25] notation, $\alpha_0 \mapsto \lambda$, $\mathsf{E} \mapsto \mathsf{S}$, $\frac{1}{2}\boldsymbol{\Omega}\wedge\mathbf{p} \mapsto \mathbf{e}.\Lambda$, where $\Lambda = \frac{1}{2}(\mathsf{G}-\mathsf{G}^T)$, and $\mathbf{p}.\mathsf{E}.(\mathsf{I}-\mathbf{pp}) \mapsto (\mathsf{I}-\mathbf{ee})\mathbf{e}:\mathsf{S}.$] In Eq. (A1), $\mathbf{F}$ is a constant external body force, typically gravity, $\mathsf{M}(\mathbf{p})$ is the translational mobility tensor, and $\mathsf{D}_T(\mathbf{p})$ is the translational diffusivity tensor. The new terms in (A1) in this paper are swimming, represented by $V_s\mathbf{p}$ in Eq. (3) and gyrotaxis given by $[\mathbf{k}-(\mathbf{k}.\mathbf{p})\mathbf{p}]/2B$ in Eq. (6). $\mathsf{D}_T(\mathbf{p}) \equiv 0$ in our case because the micro-organisms are too large to be significantly affected by Brownian motion.

Frankel and Brenner show that $\overline{\mathbf{U}}$ and $\overline{\mathsf{D}}$ can be evaluated from the integrals

$$\overline{\mathbf{U}} = \int_{S_2} P_0^{\infty}(\mathbf{p})\mathsf{M}(\mathbf{p}).\mathbf{F}d^2\mathbf{p} \tag{A4}$$

and

$$\overline{\mathsf{D}} = \int_{S_2} P_0^{\infty}(\mathbf{p})[\mathbf{B}(\mathbf{p})\mathsf{M}(\mathbf{p}).\mathbf{F}]^{\mathrm{sym}}d^2\mathbf{p} \tag{A5}$$

[Eqs. (2.8) and (2.9c) in Ref. 25]. $\mathbf{B}(\mathbf{p})$ satisfies

$$\boldsymbol{\nabla}_{\mathrm{p}}.[\dot{\mathbf{p}}P_0^{\infty}\mathbf{B} - d_{\mathrm{r}}\boldsymbol{\nabla}_{\mathrm{p}}(P_0^{\infty}\mathbf{B})] - P_0^{\infty}\mathbf{B}.\mathsf{G} = P_0^{\infty}(\mathsf{M}-\overline{\mathsf{M}}).\mathbf{F} \tag{A6}$$

[Eq. (2.19a) in Ref. 25], where

$$\overline{\mathsf{M}} = \int_{S_2} P_0^{\infty}(\mathbf{p})\mathsf{M}(\mathbf{p})\, d^2\mathbf{p}. \tag{A7}$$

The governing equations for the swimming micro-organisms follow directly from setting

$$\mathsf{M}(\mathbf{p}).\mathbf{F} \equiv \mathsf{V}_s\mathbf{p} \tag{A8}$$

and modifying $\dot{\mathbf{p}}$ to include the gyrotactic term $[\boldsymbol{k}-(\boldsymbol{k}.\mathbf{p})\mathbf{p}]/2B$.

[1] T. J. Pedley and J. O. Kessler, "Hydrodynamic phenomena in suspensions of swimming micro-organisms," Annu. Rev. Fluid Mech. **24**, 313 (1992).
[2] H. Wager, "On the effect of gravity upon the movements and aggregation of *Euglena viridis*, Ehrb., and other micro-organisms," Philos. Trans. R. Soc. London, Ser. B **201**, 333 (1911).
[3] J. B. Loeffer and R. B. Mefferd, "Concerning pattern formation by free-swimming microorganisms," Am. Nat. **86**, 325 (1952).
[4] J. R. Platt, "Bioconvection patterns in cultures of free-swimming organisms," Science **133**, 1766 (1961).
[5] J. J. Wille and C. F. Ehret, "Circadian rhythm of pattern formation in population of a free-swimming organism, *Tetrahymena*," J. Protozool. **15**, 789 (1968).
[6] M. S. Plesset and H. Winet, "Bioconvection patterns in swimming micro-organism cultures as an example of Rayleigh–Taylor instability," Nature (London) **248**, 441 (1974).
[7] S. Childress, M. Levandowsky, and E. A. Spiegel, "Pattern formation in a suspension of swimming micro-organisms: Equations and stability theory," J. Fluid Mech. **69**, 595 (1975).
[8] J. O. Kessler, "Gyrotactic buoyant convection and spontaneous pattern formation in algal cell cultures," in *Non-equilibrium Cooperative Phenomena in Physics and Related Fields*, edited by M. G. Velarde (Plenum, New York, 1984), p. 241.
[9] J. O. Kessler, "Hydrodynamic focusing of motile algal cells," Nature (London) **313**, 218 (1985).
[10] J. O. Kessler, "Cooperative and concentrative phenomena of swimming microorganisms," Contemp. Phys. **26**, 147 (1985).
[11] J. O. Kessler, "Individual and collective fluid dynamics of swimming cells," J. Fluid Mech. **173**, 191 (1986).
[12] T. J. Pedley and J. O. Kessler, "The orientation of spheroidal micro-organisms swimming in a flow field," Proc. R. Soc. London, Ser. B **231**, 47 (1987).
[13] T. J. Pedley, N. A. Hill, and J. O. Kessler, "The growth of bioconvection patterns in a uniform suspension of gyrotactic micro-organisms," J. Fluid Mech. **195**, 223 (1988).
[14] A. Harashima, M. Watanabe, and I. Fujishiro, "Evolution of bioconvection patterns in a culture of motile flagellates," Phys. Fluids **31**, 764 (1988).
[15] N. A. Hill, T. J. Pedley, and J. O. Kessler, "Growth of bioconvection patterns in a suspension of gyrotactic micro-organisms in a layer of finite depth," J. Fluid Mech. **208**, 509 (1989).
[16] T. J. Pedley and J. O. Kessler, "A new continuum model for suspensions of gyrotactic micro-organisms," J. Fluid Mech. **212**, 155 (1990).
[17] M. A. Bees and N. A. Hill, "Wavelengths of bioconvection patterns," J. Exp. Biol. **200**, 1515 (1997).
[18] N. A. Hill and D. P. Häder, "A biased random walk model for the trajectories of swimming micro-organisms," J. Theor. Biol. **186**, 503 (1997).
[19] M. A. Bees, N. A. Hill, and T. J. Pedley, "Analytical approximations for the orientation distribution of small dipolar particles in steady shear flows," J. Math. Biol. **36**, 269 (1998).
[20] S. Ghorai and N. A. Hill, "Development and stability of gyrotactic plumes in bioconvection," J. Fluid Mech. **400**, 1 (1999).
[21] S. Ghorai and N. A. Hill, "Periodic arrays of gyrotactic plumes in bioconvection," Phys. Fluids **12**, 5 (2000).
[22] S. Ghorai and N. A. Hill, "Wavelengths of gyrotactic plumes in bioconvection," Bull. Math. Biol. **62**, 429 (2000).
[23] A. M. Roberts, "Geotaxis in motile microorganisms," J. Exp. Biol. **53**, 687 (1970).
[24] I. Frankel and H. Brenner, "Generalized Taylor dispersion phenomena in unbounded homogeneous shear flows," J. Fluid Mech. **230**, 147 (1991).
[25] I. Frankel and H. Brenner, "Taylor dispersion of orientable Brownian particles in unbounded homogeneous shear flows," J. Fluid Mech. **255**, 129 (1993).
[26] R. B. Bird, R. C. Armstrong, and O. Hassager, *Dynamics of Polymeric Liquids*, Fluid Mechanics, Vol. 1, 2nd ed. (Wiley, New York, 1997).
[27] G. Arfken, *Mathematical Methods for Physicists*, 3rd ed. (Academic, New York, 1985).